Stent induced loading of the aortic valve complex

Hopf, Raoul ; Gessat, Michael ; Falk, Volkmar ; Mazza, Edoardo

Abstract: In order to evaluate the performance of stents used in transcatheter aortic valve implantation (T-AVI), finite element simulations are set up to re-construct patient specific contact forces between implant and its surrounding tissue. The reference geometry of the stent is obtained using micro-CT scanning data. A procedure is defined to create a numerically efficient and robust model of the stent made of beam elements. The model is validated with experiments applying representative loading cases. Post-op CT image data provide patient specific displacement maps used to define kinematic boundary conditions for the finite element simulation. An approach to deal with the issue of spurious strains induced by measurement uncertainties from CT images is proposed. Maps of radial forces acting on the aortic tissue are obtained.

Originally published at:
Hopf, Raoul; Gessat, Michael; Falk, Volkmar; Mazza, Edoardo (2012). Stent induced loading of the aortic valve complex. In: 15th International Conference on Medical Image Computing and Computer Assisted Intervention (MICCAI), Nice, 1 October 2012 - 5 October 2012.

Stent Induced Loading of the Aortic Valve Complex

Raoul Hopf[1,*], Michael Gessat[3], Volkmar Falk[2], Edoardo Mazza[1]

[1]Institute of Mechanical Systems, Department of Mechanical Engineering, Swiss Federal Institute of Technology (ETH), Switzerland
{rhopf, emazza}@ethz.ch
[2]Division of Cardiovascular Surgery, University Hospital Zurich, Switzerland
volkmar.falk@usz.ch
[3]Computer Vision Laboratory, Department of Electrical Engineering, Swiss Federal Institute of Technology (ETH), Switzerland
mgessat@ethz.ch

Abstract. In order to evaluate the performance of stents used in transcatheter aortic valve implantation (T-AVI), finite element simulations are set up to reconstruct patient specific contact forces between implant and its surrounding tissue. The reference geometry of the stent is obtained using micro-CT scanning data. A procedure is defined to create a numerically efficient and robust model of the stent made of beam elements. The model is validated with experiments applying representative loading cases. Post-op CT image data provide patient specific displacement maps used to define kinematic boundary conditions for the finite element simulation. An approach to deal with the issue of spurious strains induced by measurement uncertainties from CT images is proposed. Maps of radial forces acting on the aortic tissue are obtained.

Keywords: tavi, aortic stent, corevalve, simulation, contact forces

1 Introduction

Knowledge about the contact forces between a medical implant and its surrounding tissue can provide essential information on the overall performance of the implant. In particular, in the case of transcatheter aortic valve implantation (T-AVI). Insufficient contact forces between stent and tissue might cause paravalvular leaks[1]. On the contrary, excessive contact forces are suspected to impair the conductibility of the atrio-ventricular (AV) node, the bundle of His, and/or the left bundle branch. All three result in bradicaridal arrhythmia, which is a common complication after T-AVI, usually requiring pacemaker implantation[2]. The two main risk factors which could be identified as significant in clinical studies are (i) the type of valve selected for implantation and (ii) valve oversizing (resulting in high radial loads)[2,3]. These findings indicate a connection between mechanical stress induced on the tissues and the necessity for a pacemaker after T-AVI. Nevertheless, there exists no quantitative investigation of this relationship, which would allow predicting or help reducing the onset of conduction abnormalities after T-AVI.

adfa, p. 1, 2011.

In order to provide clinical research with a tool for quantitative analysis of stent-tissue interaction, for T-AVI as well as for other applications, a general concept has been developed for the reconstruction of the state of deformation of the stent as well as the contact forces between implant and tissue in-vivo.
The novel procedure (M. Gessat, V. Falk, E. Mazza, R. Hopf, Swiss/EU patent application, submitted) is based on two key elements: force balance at the stent-tissue interface and the availability of high-resolution geometrical data of the stent before and after implantation. In fact, in order to obtain the stress field at the contact points, it is sufficient to determine the boundary conditions corresponding to the measured state of deformation of the stent. Modern medical imaging systems, such as CT, provide the possibility to acquire high-resolution image data, which can be used to reconstruct deformed implant geometries in three dimensions.

An exemplary implementation of the concept is shown for the determination of contact forces between stent and tissue after T-AVI. The procedure uses geometrical data obtained from high-resolution medical imaging systems and the force field is reconstructed through finite element simulations. The present analysis is performed for the Medtronic CoreValve Revalving System (Medtronic, Minneapolis USA).

2 Methods

In a first step, a micro-CT scan of the implant is acquired from which a finite element mesh is generated corresponding to its undeformed reference configuration. Experimental validation is used to evaluate the reliability of the stent model. To obtain the actual in-vivo displacement field after implantation, postoperative CT images are analyzed. With help of this data a discrete displacement map for all junction points of the stent is obtained. This nodal displacement field is used to impose kinematic boundary conditions at the corresponding nodes of the stent model. Due to the measurement uncertainty, directly applied boundary conditions lead to high noise in the reconstructed force field. Therefore a system using nonlinear connector elements is introduced, in order to apply boundary conditions with tolerances corresponding to the limits given by measurement uncertainties. All meshing and simulation set up is carried out in MATLAB (MathWorks) and then exported in form of a finite element input file. Subsequently, simulations are solved using the program ABAQUS/standard (Dassault Systèmes Simulia Corp., Providence, RI, USA). In post processing steps (MATLAB), the reaction force field is visualized. Lower bound thresholds are set to determine zones that can be regarded as stress-free due to weak or no contact between stent and tissue.

2.1 Modeling the Reference Geometry

Stent model implementations found in current literature are mostly set up using full three dimensional solid element formulations[4,5]. Meshes using a variety of element formulations, different resolutions and integration schemes can be found. Due to the slender substructure which is largely subject to bending, tension and torque states of loading, three dimensional element formulations can yield numerical problems, such as shearlocking and hourglassing modes. In order to compare with the performance of the beam model formulation, first a full solid meshing system is implemented. This model then is used to perform a convergence study for three different states of deformation.

The geometry of the stent as extracted from CT images consists of 30 strings (Fig.1: green) and 165 intersection points (Fig.1: red). The strings have a rectangular profile with an average width and height of 0.2mm and 0.48mm. From micro-CT imaging data, Bézier splines defining the center line of each string of the undeformed stent can be fitted[6]. These splines are defined piecewise, using a 4-point control polygon. The first step in the meshing process is to discretize the string center lines as shown in Fig 1. The sampling rate to generate the center line nodes is adjustable.

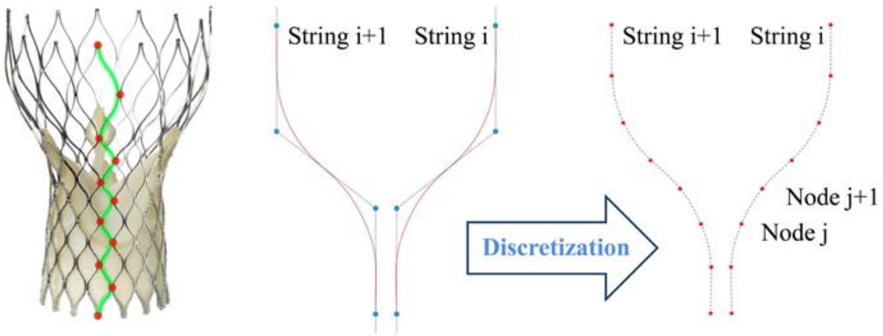

Fig. 1. Stent including leaflets (not modeled) with highlighted a string (green) and according intersection points (red). Bézier-control polygons and discretized center lines.

One of the main difficulties in meshing three dimensional structures with beam elements is to maintain correct orientation for all elements with respect to the geometry and the norm of the finite element solving system that is used. For this purpose, every node on the center line is provided with a local coordinate system, that holds the tangent vector of the spline and two normal vectors which form an orthonormal, right-handed trihedron. The tangents can directly be obtained from the definition of the Bézier splines. The outward normal is calculated from a global cylindrical coordinate system and the tangent, whereas the second normal is obtained from the first two vectors.
The beam element model requires the discretized center lines of the strings and the definition of a cross section. The chosen elements for this model are three dimensional first order two point Timoshenko beam elements (element type B31 in ABAQUS). In order to avoid initial twists or curvatures, both starting- and endpoint of the element need to be provided with the corresponding tangent- and normal vectors. These are obtained by interpolating the vectors which were used to define the nodal coordinate systems. At each intersection point, both corresponding nodes of the neighboring strings are coupled using kinematic equations in all six degrees of freedom.

For the solid model the cross section is discretized in a plane reference system and then transformed into the according local nodal systems. The nodes are connected to form first order, hexahedral solid elements and a reduced integration scheme is applied (element type C3D8R in ABAQUS).

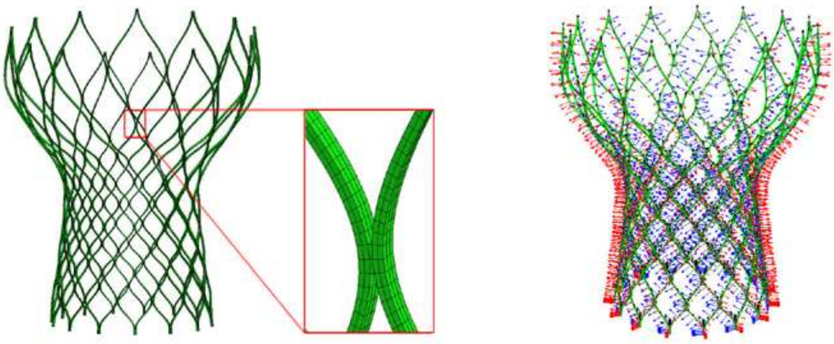

Fig.2. Solid model (left) with a close up view of the mesh (middle). Beam element model (right) with rendered beam profiles and element orientation vectors.

The material used in CoreValve is a nickel-titanium alloy (Nitinol), which exhibits super elastic properties to be able to fully recover from strains of up to 10% as a result of the stents crimping process to the catheter. The constitutive model used for the present study is a linear elastic Hookean solid. In fact, the crimping process is not included in the analysis and, the final deformed state of the stent may include finite rotations but deformation is expected to remain in the small strain regime. Overestimation of stiffness due to choosing a linear elastic model was observed when comparing with experimental data at large deformations, see section 2.3.

2.2 Evaluation of the Influence of Mesh Size

The convergence study is performed using four mesh resolutions ranging from orders of 10'000 (grade 1) to 600'000 (grade 4) elements for the solid model. Approximately 4'000 elements are used for the beam model. Three different global loading states are tested. Fig. 3 shows the results of the analysis of mode 1 loading (global tension) for the four mesh configurations of the solid model. Mode 2 was defined as a global compression and mode 3 a torsional state. The results of modes 2 and 3 are consistent with Fig. 3. An important remark concerns the result of grade 1. Due to the low mesh resolution the profile has only one element in the cross section. The reduced integration scheme for first order elements in states of bending therefore lead to zero-energy deformation modes (hourglassing), which yields completely unrealistic results as seen in Fig. 3. The same deformation modes were applied to the beam element model which provides results for all modes comparable with grades 3 and 4, but with only around 25'000 degrees of freedom.

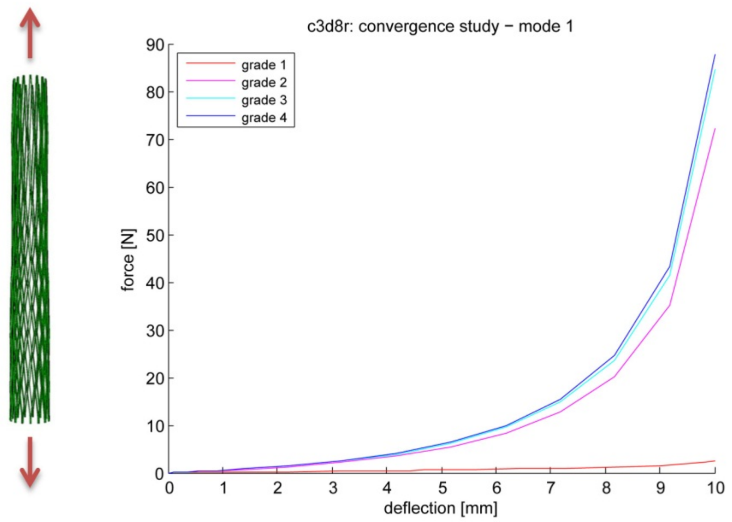

Fig. 3. Mode 1 and results of the corresponding analysis for all mesh resolutions.

2.3 Experimental Validation

The experimental validation of the beam model is performed with one dimensional two point tensile tests. Three configurations were investigated: One symmetrical mode and two nonsymmetrical modes (mode 1 shown in Fig. 4).

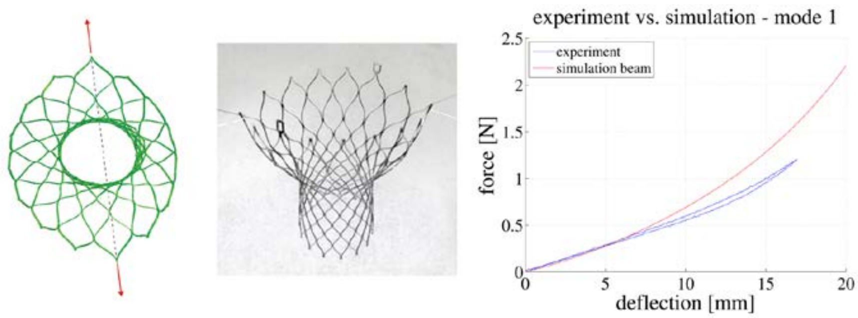

Fig. 4. Mode 1: FE-model, experiment, measured curve (blue) and simulation (red).

Such experiments are relatively easy to perform and mechanically well defined in terms of boundary conditions. In spite of the one dimensional boundary conditions, the coupled grid structure of the stent leads to complex states of deformation, which test both structural as well as constitutive model reliability.

Simulations show good predictive capabilities for low to moderate deflections but a clear overestimation of stiffness for larger deformations. This is deemed to be a consequence of the chosen linear elastic constitutive model. The super elastic material behavior of Nitinol shows lower stresses at the corresponding level of deformations imposed in the experiments.

2.4 Boundary Conditions for Postoperative Simulation

In order to obtain a patient-specific measurement for the deformation of the CoreValve stent after implantation, a sparsely sampled deformation field is generated. Therefore, the 165 intersection points which define the stent's grid structure are automatically extracted from CT images. With a high spatial resolution (< 0.4 mm in all axes), these intersection points are well visible in CT images as small, well-defined clusters of high-intensity voxels due to the high X-ray contrast of Nitinol. Nevertheless, calcium clusters and image artifacts can create similar clusters or create enough background noise to merge neighboring clusters. A combination of threshold filtering and model-based generation of hypotheses for likely positions of these intersection points is applied in order to identify the intersection points. In practical tests with 25 patient datasets, the proposed method has proved reasonably robust to image noise and calcium. Due to sampling effects and image blurring, the spatial accuracy of the landmark localization was evaluated to be in the range of two voxel lengths, i.e. 0.8 mm.

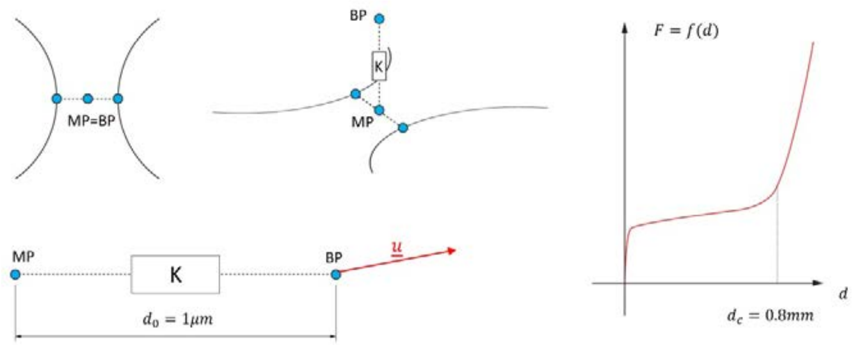

Fig. 5. Intersection middle point (MP), boundary point (BP), connector element (K) and the corresponding nonlinear force law.

If this deformation map was be used directly to impose kinematic boundary conditions at the intersection points, the high ratio of tensile to bending stiffness in beam-like structures would yield large fluctuations in the values of calculated external forces, due to inaccuracy in intersection point position measurement. Therefore an intermediate step was introduced in order to relax these spurious forces. The proposed method is illustrated in Fig. 5. A middle (MP) point is calculated for each intersection. An additional boundary point (BP) in radial direction towards the center of the stent is created. The distance between MP and BP in the undeformed configuration is by orders of magnitude smaller than the applied displacements.. The middle point and the boundary point are connected with a nonlinear force element (K). The force law for the connector element is set up to have a cut-off at approximately d_c=0.8 mm, which corresponds to the uncertainty of the CT-data. The measured displacement is now applied at the boundary point, instead of the middle point directly. This allows the actual physical middle points to position themselves within a spherical volume around the nominal position to account for measurement uncertainty, thus leading to a global minimum of potential energy in the stent. This approach avoids artificially high reaction forces and provides a lower limit for the actual force field acting on the stent in-vivo.

3 Results

The discrete vector field containing the nodal reaction forces of each intersection point is imported into MATLAB for post processing. The radial components of the forces can be represented as arrows in a three dimensional plot, or their values reported for all nodes along selected paths, as shown in Fig. 6. The green dots correspond to the plotted arrows at nodes 1-7 in the diagram. The sign of the nodal plot was chosen to indicate whether the force points radially inward or outward. Reaction forces in outward direction are considered as artifacts, since the surrounding tissue will not exhibit any adhesion properties in comparable magnitudes. These negative contact forces possibly indicate a local underestimation of the measurement uncertainty in the post-op CT data.
The average value of radial force divided by the corresponding aortic tissue area, typically yields a radial pressure in the range of 30-40 mbar. These stress levels seem plausible when compared with the average values of blood pressure fluctuation between systolic and diastolic pressure (approx. 50 mbar).

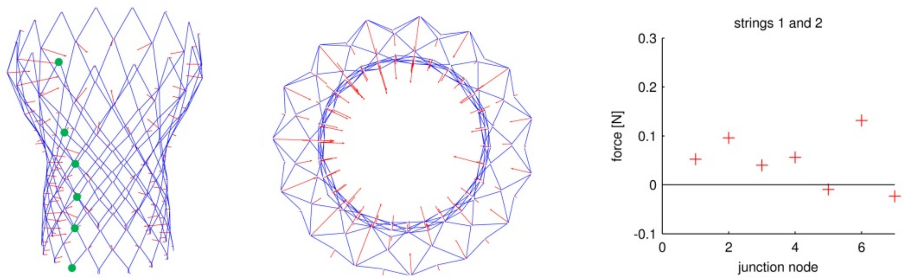

Fig. 6. Three dimensional plot of the force field and nodal force plot.

4 Conclusions

An effective beam model of the CoreValve aortic stent has been created, compared to solid element models and validated experimentally. A method to extract a patient specific nodal deformation map from medical imaging data and a corresponding procedure to deal with measurement uncertainty have been developed. The model performed well in terms of efficiency as well as robustness and showed good predictive capabilities in low to moderate ranges of displacement corresponding experiments.

The feasibility of the novel procedure for reconstruction of stent-tissue interaction from medical images of in-vivo stent deformation has been demonstrated. Previous studies using finite element simulation for post-operative outcomes have used medical imaging systems to obtain patient specific data[4,5,7,8]. This data was then used to either model patient specific vascular geometries, or to obtain global information of the implanted stent. However, to the best of our knowledge so far procedure exists to obtain contact forces between stent and tissue from post-op data.
The application of displacement boundary conditions needs further investigation to minimize the artifacts related to measurement uncertainties and avoid local underestimation of contact forces. Further, considering future applications that involve the crimping and releasing processes, a non-linear constitutive model has to be implemented able to reproduce the super elastic properties of Nitinol.

5 Acknowledgements

The project was supported by the Swiss National Science Foundation (SNSF, project nr: CR32I3 135044) and the Swiss Heart Foundation.

6 References

1. M. Padala, E.L. Sarin, P. Willis, V. Babaliaros, P. Block, R.A. Guyton und V.H. Thourani, An engineering review of transcatheter aortic valve technologies. Cardiovasc. Eng. Technol. 1:77-87, 2010.
2. M.Z. Khawaja et al., Permanent pacemaker insertion after CoreValve transcatheter aortic valve implantation: incidence and contributing factors (the UK CoreValve collaborative). Circulation 123:951-960, 2011.
3. J.M. Bosmans et al., Procedural, 30-day and one year outcome following CoreValve or Edwards transcatheter aortic valve implantation: results of the Belgian national registry. Interact. Cardiovasc. Thorac. Surg. 12:762-767, 2011.
4. C. Capelli, G.M. Bosi et al., Patient-specific simulations of transcatheter aortic valve stent implantation, Med. Biol. Eng. Comput. (2012) 50:183–192
5. Tzamtzis S, et al. Numerical analysis of the radial force produced by the Medtronic-CoreValve and EdwardsSAPIEN after transcatheter aortic valve implantation (TAVI). Med Eng Phys (2012)
6. M. Gessat, L. Altwegg, T. Frauenfelder, A. Plass, V. Falk, Cubic hermite bezier spline based reconstruction of implanted aortic valve stents from CT images, Proc. of the 33rd Annular International Conference of the IEEE Enginnering in Medicine and Biology Society (EMBC) 2011, August 2011
7. A. Ganguly, R. Simons et al., In-vitro imaging of femoral artery nitinol stents for defmation analysis. J Vasc Interv Radiol. 2011 Feb;22(2):236-43.
8. A. Ganguly, R. Simons et al., In-vivo imaging of femoral artery nitinol stents for deformation analysis. J Vasc Interv Radiol. 2011 Feb;22(2):244-9.